

Laser and Thermal Vapor Deposition of Metal Sulfide (NiS, PdS) Films and in Situ Gas-Phase Luminescence of Photofragments from $M(S_2COCHMe_2)_2$

Jinwoo Cheon, David S. Talaga, and Jeffrey I. Zink*

Department of Chemistry and Biochemistry, University of California,
Los Angeles, California 90095

Received November 15, 1996. Revised Manuscript Received January 29, 1997[®]

NiS and PdS thin films are prepared at 10^{-2} Torr from the single-source precursors $M(S_2COCHMe_2)_2$, $M = Ni$ and Pd . Two different vapor deposition processes, photochemical and thermal, are employed. Gas-phase emission spectroscopy is used during the photochemical deposition to identify the two elemental components of the final materials, the metal atom and sulfur, in the gas phase. NiS and PdS thin films are grown by the thermal process at 300 and 350 °C, respectively, on Si and quartz substrates. The NiS films are highly oriented rhombohedral (γ) phase, and the PdS films are tetragonal-phase polycrystalline. The metal sulfide films are grown photolytically by 308 nm laser irradiation of the gas-phase precursors at lower temperatures (near the sublimation temperature). The NiS films show no X-ray diffraction patterns, but the PdS films are polycrystalline tetragonal phase. The films are analyzed by various surface analytical tools including scanning electron microscopy, X-ray photoelectron, and Rutherford backscattering techniques.

Introduction

Laser-driven photochemical vapor deposition (LCVD) of thin-film materials is an area of current interest because of the unique processing advantages such as spatially selective deposition (patterning) and selective energy transfer to the precursors.^{1,2} Real time patterning of desired materials on substrates is possible at relatively low temperatures.³ The light-driven photofragmentation reactions involved in this process are poorly understood. Spectroscopic studies carried out during deposition are of importance in order to identify photofragments and understand the fundamental steps during laser deposition. When light emission is observed, luminescence spectroscopy can serve as an in situ optical probe of the photofragments. We have recently employed this technique to study laser-driven CVD processes of semiconductor films (ZnS)⁴ from metal xanthate precursors and metal films (Cu, Au)^{5,6} from hexafluoroacetylacetonate precursors.

In the only reported spectroscopic study of photofragments produced during metal sulfide film deposition, both of the components of the final film, metal atoms and sulfur, were observed spectroscopically in the gas phase.⁴ The precursor in that study was the bis(isopropylxanthate) zinc complex $Zn(S_2COCHMe_2)_2$. To investigate the possible generality of this fragmentation mode in the photodeposition of metal sulfide films, bis-

(isopropylxanthate) complexes of nickel and palladium were chosen. Nickel sulfide (NiS) has the interesting electromagnetic property of a first-order phase transition from a low-temperature antiferromagnetic semiconductor to a high-temperature paramagnetic metal.^{7–9} Other applications of NiS include its use as a hydrodesulfurization catalyst¹⁰ and as a cathodic material.¹¹ A variety of nickel sulfide powder compositions (e.g., NiS, Ni_3S_2) have been prepared by the mechanical alloying technique where elemental mixtures of Ni and S are milled in a high-energy shaker.¹² Stoichiometric NiS films have been grown by pulsed laser ablation of Ni:S targets with composition ratios in the range 1–3.¹³ The films consisted of a mixture of hexagonal (β -phase) and/or rhombohedral (γ -phase) NiS depending on the target composition. The palladium sulfide materials are semiconductors ($E_g = \sim 2$ eV) and have been studied as a constituent of a ternary phase (e.g., Pd–P–S) catalytic photoelectrode.¹⁴

In this paper, we report the laser-driven photochemical vapor deposition of NiS and PdS films from the corresponding metal isopropyl xanthate complexes, bis(*O*-isopropylthiocarbonato)nickel(II) and -palladium(II), $M(S_2COCHMe_2)_2$, $M = Ni, Pd$. The solid-state thermochemistry of transition-metal xanthate compounds has been widely investigated; these compounds decompose into inorganic metal sulfide along with

[®] Abstract published in *Advance ACS Abstracts*, March 15, 1997.

(1) Herman, I. P. *Chem. Rev.* **1989**, *89*, 1323.
(2) Eden, J. G. *Photochemical Vapor Deposition*; Wiley: New York, 1992.
(3) *Laser Chemical Processing for Microelectronics*; Ibbs, K. G., Osgood, R. M., Eds.; Cambridge University: Cambridge, 1989.
(4) Cheon, J.; Talaga, D. S.; Zink, J. I. *J. Am. Chem. Soc.* **1997**, *119*, 163.
(5) Wexler, D.; Zink, J. I.; Tutt, L. W.; Lunt, S. R. *J. Phys. Chem.* **1993**, *97*, 13563.
(6) Talaga, D. S.; Zink, J. I. *Inorg. Chem.* **1996**, *35*, 5050.

(7) Alder, D. *Rev. Mod. Phys.* **1968**, *40*, 714.
(8) Sparks, J. T.; Komoto, T. *Rev. Mod. Phys.* **1968**, *40*, 752.
(9) Lioutas, Ch. B.; Manolikas, C.; Van Tendeloo, G.; Van Landuyt, J. *J. Cryst. Growth* **1993**, *126*, 457.
(10) Startsev, A. N.; Shkurovat, S. A.; Zaikovskii, V. I.; Moroz, E. M.; Ermakov, Yu. I.; Plaksin, G. V.; Tsekhanovich, M. S.; Surovikin, V. F. *Kinet. Katal.* **1988**, *29*, 398.
(11) Tilak, B. V.; Ramamurthy, A. C.; Conway, B. E. *Proc. Indian Acad. Sci. Chem. Sci.* **1986**, *97*, 359.
(12) Kosmac, T.; Maurice, D.; Courtney, T. H. *J. Am. Ceram. Soc.* **1993**, *76*, 2345.
(13) Lee, H.; Kana, M.; Kawai, T.; Kawai, S. *Jpn. J. Appl. Phys. Part 1* **1993**, *32*, 2100.

various organic byproducts upon heating.¹⁵ However, there has been no attempt to grow metal sulfide thin films by vapor deposition processes. In particular, Pd and Ni isopropyl xanthate compounds are volatile enough to be used for our vapor deposition studies. These metal xanthate compounds have a distorted square-planar geometry defined by four S atoms from the chelating xanthate ligands.¹⁶ Very little is known about the photochemistry of metal xanthate compounds, but photoactivated ligand dissociation processes are known for metal complexes with analogous dithiocarbamate ligands.^{17,18} In this study, metal sulfide films are prepared by both thermal and laser-driven CVD processes, and the film properties are compared. Light emission is observed during the deposition process, and gas-phase photoluminescence spectra are recorded and analyzed to identify photoproducts.

Experimental Section

Materials and General Methods. Metal isopropyl xanthate compounds, $M(S_2COCHMe)_2$; $M = Ni, Pd$, were prepared by the stoichiometric reaction of potassium isopropylxanthate and the metal nitrate (or chloride) following the literature methods.^{19–21} After recrystallization from $CHCl_3$ and characterization by 1H NMR and mass spectroscopy (E.I.), they were used for CVD and gas-phase experiments.

The thin films were characterized by various surface analytical tools. X-ray powder diffraction (XRD) patterns were acquired using $Cu K\alpha$ radiation with a power supply of 40 kV and 30 mA. Scanning electron micrographs were obtained on a Cambridge Stereo Scan 250 instrument. X-ray photoelectron spectra were obtained with a 15 kV, 400 W Al $K\alpha$ radiation source (1486.6 eV) under an operation pressure of ca. 10^{-9} Torr. The surfaces of the films were cleaned by Ar^+ sputtering of the films for 3–5 min (corresponding to roughly 20–30 nm in depth), and the amount of carbon and oxygen contamination was estimated by considering sensitivity factors.²² Rutherford backscattering (RBS) was obtained using a 1.8 MeV He ion beam with a silicon surface barrier detector located at 165° with respect to the ion beam.

Thermal CVD. The thermal CVD experiments were conducted at $\sim 10^{-2}$ Torr in a hot-wall horizontal Pyrex tube where two different temperature regions (sublimation and deposition) are regulated by external heating tape. The precursor was sublimed directly into the cell without using any carrier gas. The vacuum was maintained by a standard mechanical rotary pump. The precursor (~ 0.1 g) was introduced into the film-growth region, and deposition occurred on the substrates (Si wafers, quartz slides) and on the inner surface of the reactor wall at $350^\circ C$ for PdS and $300^\circ C$ for NiS. The sublimation temperature for the Ni precursor was $95^\circ C$, and that for Pd precursor was $105^\circ C$. The gold-colored NiS films and silver-colored PdS films were smooth and reflective. Typical growth times were 3 h, and about $0.7 \mu m$ thick NiS and $0.5 \mu m$ thick PdS films were obtained. The estimated average growth rates were ca. 3.3 and 2.4 nm/min for the NiS and PdS films, respectively. No attempts were made to optimize the deposition rate.

Photolytic CVD. Laser-driven photodeposition was carried out at $\sim 10^{-2}$ Torr using a XeCl excimer laser (308 nm). The metal xanthate precursor (~ 0.1 g) in a reservoir cell was heated to its sublimation temperature and introduced into a CVD glass cell with quartz windows. The photodeposition was carried out by irradiating a 2 cm diameter circle on substrates (Si wafers, quartz slides) with 30 mJ/pulse at 20 Hz for a resulting fluence of $\sim 1 MW cm^{-2}$. The shiny films formed exclusively on the irradiated area. Typical growth times were 3 h, and about $0.4 \mu m$ thick NiS and $0.3 \mu m$ thick PdS films were obtained. The estimated average growth rates were ca. 2 and 1.4 nm/min for the NiS and PdS films, respectively. No attempts were made to optimize the deposition rate.

Luminescence Spectroscopy. Luminescence experiments are carried out in an evacuated stainless steel 6-way cross with synthetic fused silica windows. A sample of the precursor is placed in the sample chamber and is leaked into the photolysis chamber with a needle valve. The gas-phase luminescence spectra were obtained by exciting the gas-phase sample with 308 nm radiation from a XeCl excimer laser (Lambda Physik EMG 201 MSC) under various pressure conditions (e.g., dynamic vacuum (10^{-2} Torr), static vacuum, and Ar buffer gas (~ 1 –1000 Torr)). The pulse energy used for excitation of the CVD precursors is approximately 3 mJ and the resulting fluence is typically $\sim 3 MW/cm^2$. The focused output of the laser excites the gaseous sample, and the emitted light is collected at right angles and directed into a 0.32 m single monochromator (JY HR320) where it is dispersed by a 300 or 600 groove/mm holographic grating and detected by a UV-intensified diode array detector (EG&G Princeton Applied Research OMA3 1024 \times 1). Complete details of this experimental setup were described elsewhere.⁴

Results and Discussion

1. Film Properties. NiS Thin Films by CVD. The precursor, $Ni(S_2COCHMe)_2$, is sublimed at $95^\circ C$ into CVD cell under vacuum ($\sim 10^{-2}$ Torr) and NiS films are grown at $350^\circ C$ on Si wafer and quartz slides. The gold-colored films are smooth and reflective. XPS analysis of the films reveals that the surface is highly contaminated with oxygen ($\sim 25\%$) and carbon ($\sim 30\%$) after a few days of exposure to the atmosphere. Upon Ar^+ sputtering of the films, the oxygen and carbon content dramatically decreases to less than a few atomic percent ($\sim 4\%$ for C and $\sim 3\%$ for O), and no other impurities are detected in the films. It is believed that the majority of the C and O impurities originate from the surface contamination in the atmosphere since the amounts of the impurities are much higher near the surface. X-ray diffraction studies indicate that the films are γ -phase polycrystalline with preferred orientation (Table 1). A strong peak observed at $32.20 (2\theta)$ is assigned as a rhombohedral (γ) phase (300) diffraction. Scanning electron micrographs (SEM) show that the films consist of small granules ($\sim 0.4 \mu m$ in diameter, Figure 1A).

Laser photodeposition is carried out from same precursor at 10^{-2} Torr by using 308 nm irradiation. The precursor (~ 0.1 g) is heated to its sublimation temperature and introduced into a CVD cell with quartz windows. Reflective dark gray films are formed on the substrates *exclusively* in the 2 cm diameter irradiated circle suggesting that the deposition process involves a photochemical component. XPS analysis after Ar^+ sputtering shows NiS with carbon ($\sim 5\%$) and oxygen ($\sim 2\%$) (Figure 2A). SEM indicates that the films are smooth and featureless (Figure 1B). The films show no diffraction pattern upon X-ray diffraction analysis and may exist in an amorphous phase. RBS yields elemental information representative of the entire thickness of the film, with a quantitative accuracy estimated at

(14) Folmer, J. C. W.; Turner, J. A.; Parkinson, B. A. *J. Solid State Chem.* **1987**, *68*, 28.

(15) Hill, J. O.; Murray, J. P.; Patil, K. C. *Rev. Inorg. Chem.* **1994**, *14*, 363.

(16) Tiekink, E. R. T.; Winter, G. *Rev. Inorg. Chem.* **1992**, *12*, 183.

(17) Schwendiman, D. F.; Zink, J. I. *J. Am. Chem. Soc.* **1976**, *98*, 4439.

(18) Given, K. W.; Mattson, B. M.; McGuiggan, M. F.; Miessler, G. L.; Pignolet, L. H. *J. Am. Chem. Soc.* **1977**, *99*, 4855.

(19) Rao, S. R. *Xanthate and Related Compounds*; Dekker: New York, 1971.

(20) Sceney, C. G.; Hill, J. O.; Magee, R. J. *Thermochim. Acta* **1973**, *6*, 111.

(21) Cavell, K. J.; Sceney, C. G.; Hill, J. O.; Magee, R. J. *Thermochim. Acta* **1973**, *5*, 319.

(22) *Handbook of X-ray Photoelectron Spectroscopy*; Muilenberg, G. E., Ed.; Perkin-Elmer: Eden Prairie, MN, 1978.

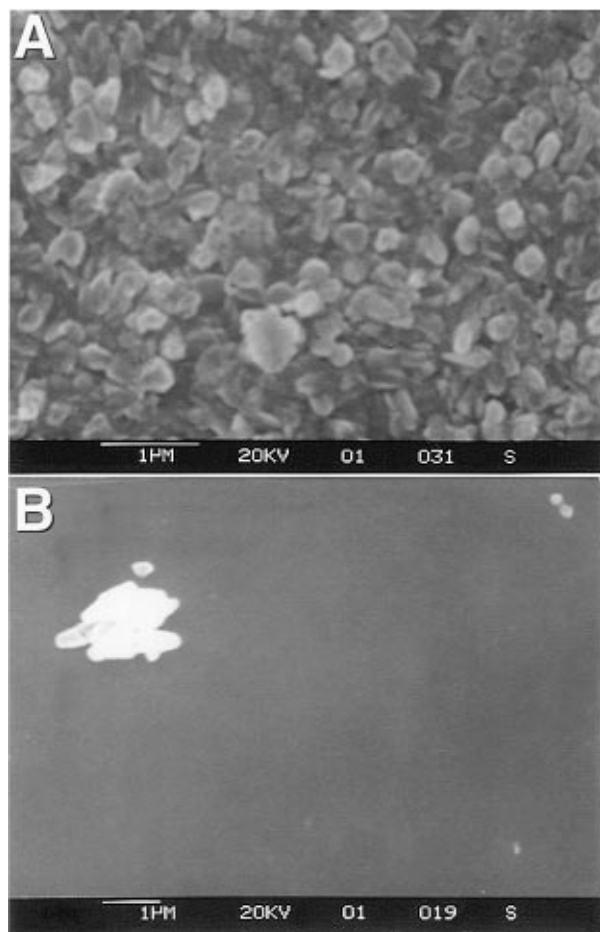


Figure 1. Scanning electron micrographs of NiS films grown on Si(111) by (A) thermal and (B) photolytic CVD. The object in the upper left side is dust.

Table 1. X-ray Diffraction Patterns of NiS and PdS Thin Films

(hkl)	2θ (deg)	(I/I ₀) observed	(I/I ₀) ref 27
NiS Grown by the Thermal Process			
(101)	30.30	0.17	0.40
(300)	32.20	1.00	1.00
(021)	35.70	0.12	0.65
(220)	37.40	0.10	0.12
(211)	40.50	0.07	0.55
(131)	48.90	0.06	0.95
PdS Grown by the Thermal Process			
(210)	31.13	1.00	0.91
(211)	33.90	0.06	1.00
PdS Grown by the Photolytic Process			
(102)	30.50	1.00	0.71
(210)	31.15	0.82	0.91
(112)	33.62	0.39	0.48
(211)	34.14	0.53	1.00

±5%. RBS analysis shows that the films have almost stoichiometric NiS composition. A slight excess of sulfur (~3 atomic %) may be present, but is just within experimental uncertainty.

PdS Thin Films by CVD. Similar thermal and photolytic CVD experiments are carried out at 10^{-2} Torr by using the $\text{Pd}(\text{S}_2\text{COCHMe}_2)_2$ precursor. The precursor is sublimed into the CVD cell at 105 °C, and PdS films were grown at 300 °C on Si wafers and quartz slides. The films are reflective and silvery. X-ray diffraction studies indicate that the films are highly oriented tetragonal-phase polycrystalline PdS (Table 1). XPS analysis confirms that Pd and sulfur are present along with oxygen (~2%) and carbon (~4%). SEM

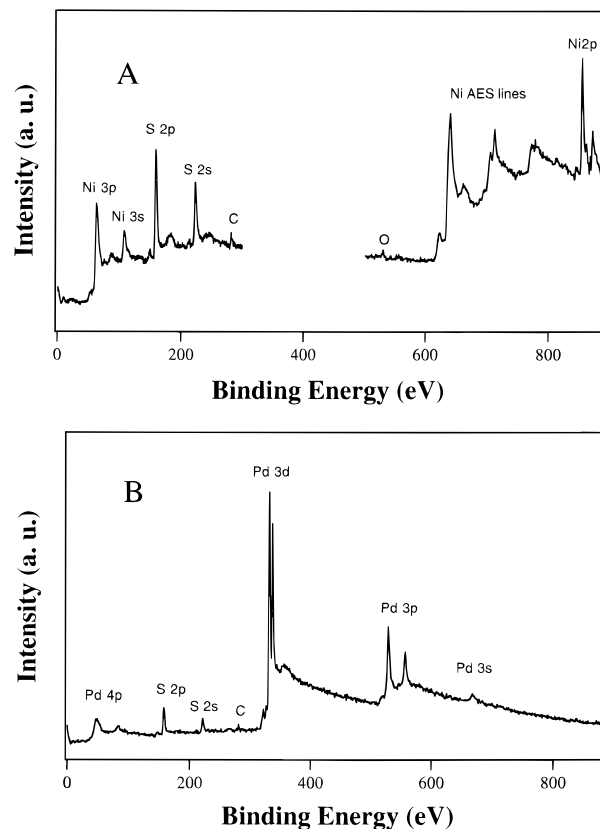


Figure 2. X-ray photoelectron spectra: (A) NiS grown on Si(111) by photolytic CVD, (B) PdS grown on Si(111) by photolytic CVD.

shows that the films are smooth with small granular islands (~130 nm in diameter, Figure 3A).

In the photolytic CVD process, dark gray films are obtained only on laser-irradiated parts of the substrate and on the quartz window where the laser beam passes through. The diffraction pattern of the films shows nonoriented polycrystalline tetragonal PdS (Table 1). The purity of the films is characterized by XPS. After Ar^+ sputtering, most of the carbon and oxygen surface contamination is removed, and PdS was identified with a peak from carbon (~5%) and no peaks from oxygen (Figure 2B). SEM shows that the films are smooth with shallow circular domes (~5–7 μm in diameter) randomly present on the flat surface (Figure 3B).

2. In Situ Luminescence from Photofragments during Photolytic CVD. During the laser-assisted CVD studies, we observe luminescence in the path of the laser beam in the cell. The emission spectra show that the luminescence originates from gas-phase photofragments and not from the intact precursor molecule (vide infra). This luminescence technique provides real-time information about the gas-phase chemical species present during the CVD process. By using gating techniques to separate the spectra of short- and long-lived species, it is possible to identify many of the photofragments and to use the information to develop an understanding of the photofragmentation pathways.

The luminescence spectrum of $\text{Ni}(\text{S}_2\text{COCHMe}_2)_2$ observed during the deposition process exhibits two main features as shown in Figure 4A. These features are separated by time-resolved gated experiments. The gated spectrum obtained during the 10 ns period that the laser pulse is on shows intense and congested bands from 330 to 370 nm. These bands are due to Ni atomic

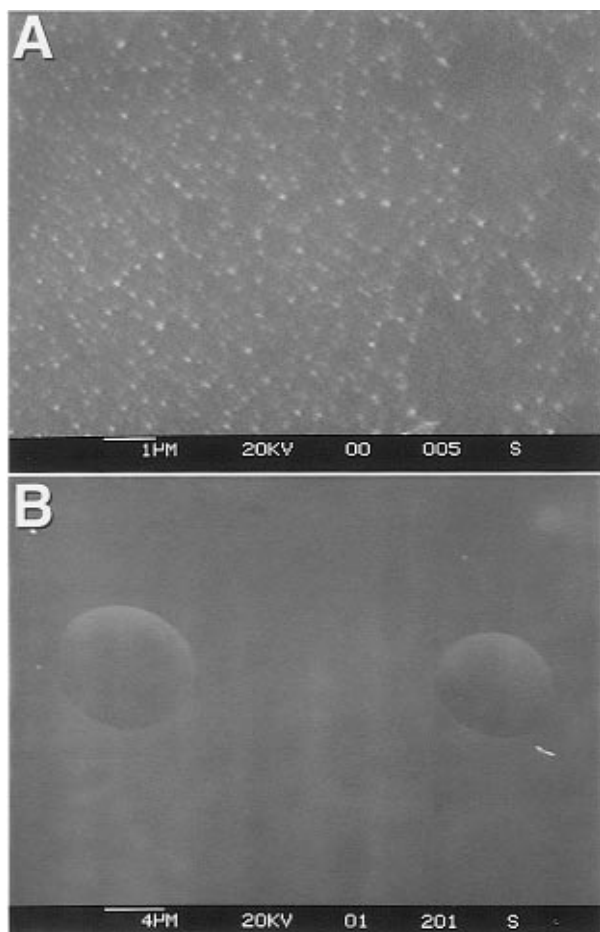


Figure 3. Scanning electron micrographs of PdS films grown on Si(111) by (A) thermal and (B) photolytic CVD.

emission (Figure 4B).²³ Less intense broader, regularly spaced bands ($\sim 720\text{ cm}^{-1}$ spacing) from 310 to 570 nm other than Ni atomic peaks (marked as with asterisks) are assignable to vibrationally hot S_2 as shown in the top trace of Figure 4C. The top trace of Figure 5 shows that the time resolved spectrum (delayed 80 ns after the laser pulse and integrated for $10\text{ }\mu\text{s}$ thereafter) in the presence of added argon buffer gas ($\sim 200\text{ mbar}$) contains a congested progression from 340 to 500 nm which also originates from S_2 .²⁴ The bottom trace of Figure 5 shows a calculated B \rightarrow X luminescence including contributions from $v = 0, 1, 2$ in the excited states that match the observed S_2 luminescence.

In the case of PdS photodeposition, very similar luminescence results are obtained. The in situ luminescence spectrum also consists of two main features shown in the middle trace of Figure 6. Characteristic Pd atomic emission lines are observed in this spectrum as compared to known atomic lines (bottom trace of Figure 6).²³ There is considerable overlap between Pd atomic lines and S_2 bands, but a few nonoverlapping Pd atomic lines could be identified (labeled with asterisks). Rather weak and broader hot S_2 bands ($\sim 720\text{ cm}^{-1}$ spacing, from 310 to 570 nm) are the major features along with Pd atomic lines in the spectrum. The middle trace of Figure 5 shows that the time-

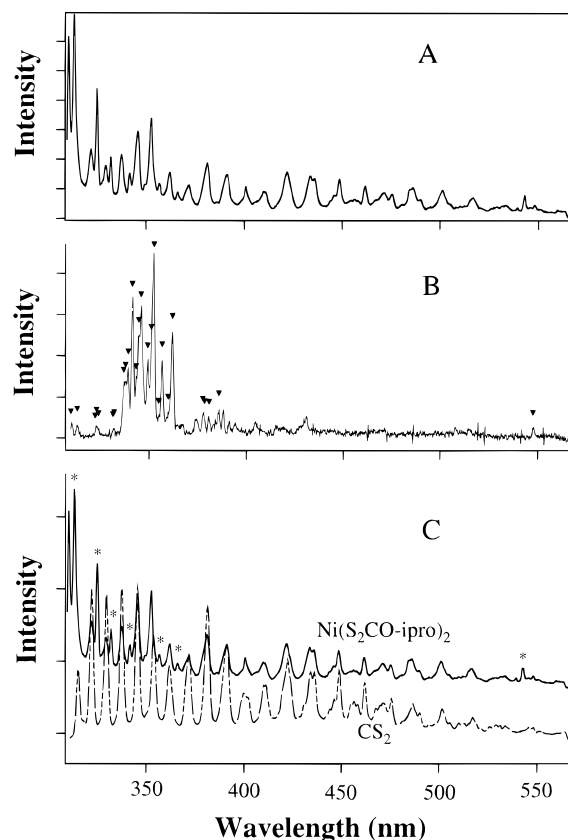


Figure 4. (A) In situ luminescence spectrum observed during photolytic CVD of $\text{Ni}(\text{S}_2\text{COCHMe}_2)_2$. (B) Gated spectrum observed under low-pressure conditions for the 10 ns during the laser pulse. Positions of known Ni atomic emission lines are shown with triangles. (C) The upper trace is the spectrum observed under low-pressure CVD conditions. The lower trace is the spectrum observed from CS_2 under identical photolytic CVD conditions.

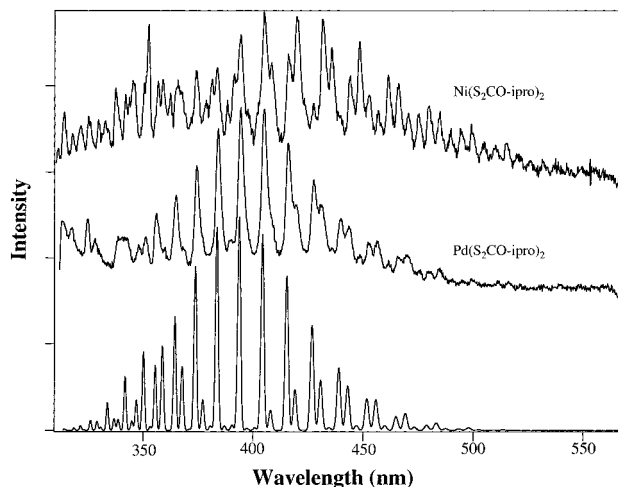


Figure 5. Top trace: spectrum observed from $\text{Ni}(\text{S}_2\text{COCHMe}_2)_2$ under high-pressure conditions delayed 80 ns after the laser pulse and integrated for $10\text{ }\mu\text{s}$ thereafter (collisionally cooled S_2 emission). Middle trace: spectrum obtained from $\text{Pd}(\text{S}_2\text{COCHMe}_2)_2$ under the same conditions as above. Bottom trace: simulated spectrum of the S_2 B \rightarrow X luminescence.

resolved spectrum (delayed 80 ns after the laser pulse and integrated for $10\text{ }\mu\text{s}$ thereafter) in the presence of added argon buffer gas ($\sim 200\text{ mbar}$) contains a congested progression from 340 to 500 nm which is assigned to the S_2 B \rightarrow X state emission.

3. Mechanistic Aspects of the Photodriven CVD in the Gas Phase. The production of metal atoms in the gas

(23) *Wavelength and Transition Probabilities for Atoms and Atomic Ions*, U.S. Department of Commerce, National Bureau of Standards: U.S. Government Printing Office: Washington, DC, 1980; NSRDS-NBS 68.

(24) Pearse, R. W. B.; Gaydon, A. G. *The Identification of Molecular Spectra*; Chapman and Hall: London, 1976.

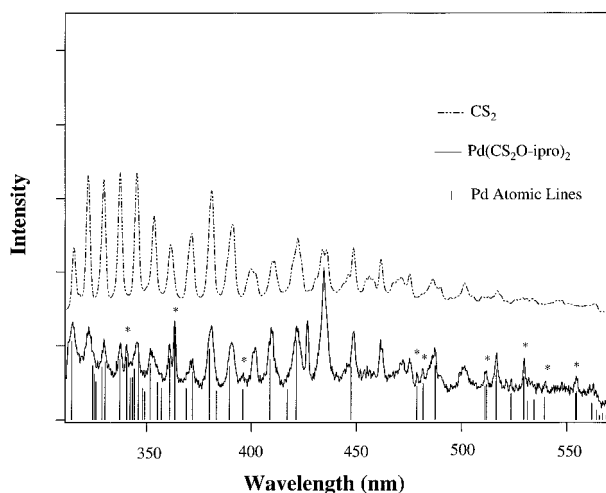


Figure 6. Middle trace: *in situ* luminescence spectrum observed during photolytic CVD of $\text{Pd}(\text{S}_2\text{COCHMe}_2)_2$. Bottom trace: positions of known Pd atomic emission lines. Top trace: spectrum observed from CS_2 under identical photolytic CVD conditions.

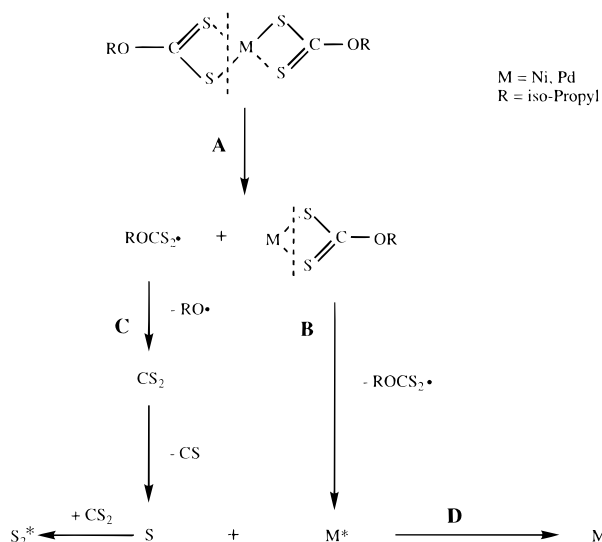


Figure 7. Photochemically activated fragmentation processes of $\text{M}(\text{S}_2\text{COCHMe}_2)_2$ ($\text{M} = \text{Ni}, \text{Pd}$) which produce M atom and S_2 luminescence and finally form metal sulfide.

phase involves multiple ligand dissociations. The first step of the fragmentation process is a ligand-to-metal charge transfer (LMCT), which possibly generates $\text{M}(\text{S}_2\text{COCHMe}_2)$ ($\text{M} = \text{Ni}, \text{Pd}$) and a xanthate radical (path A of Figure 7).²⁵ There have been reports on analogous photoactivated ligand dissociation processes for metal dithiocarbamate complexes that involve homolytic cleavage of the $\text{M}-\text{S}$ bond.^{17,18} Absorption of another photon results in further photofragmentation of the intermediate $\text{M}(\text{S}_2\text{COCHMe}_2)$ to produce another xanthate radical and a Ni or Pd atom (path B of Figure 7). The luminescence of the metal atoms probably occurs because they are produced in excited electronic states.

The emission from S_2 in the gas-phase arises from fragmentation steps involving the xanthate radical. The xanthate radical ($\bullet\text{S}_2\text{COCHMe}_2$) can fragment yielding CS_2 and an isopropoxyl radical (path C of Figure 7).

Absorption of a UV photon by CS_2 results in fragmentation yielding CS and S. The S atom can further react with CS_2 to produce luminescent S_2 .²⁶ The low-pressure spectra from fragmentation of the metal xanthate complexes shows features assignable to very hot S_2 ($\text{B} \rightarrow \text{X}$).²⁴ The spectrum from S_2 observed under higher pressure conditions with added Ar buffer gas shows substantial cooling as a result of collisions (top and middle traces of Figure 5). Our photofragmentation control study of CS_2 under identical conditions to those used for the metal xanthate complexes reproduces all of the nonmetal features present in the metal xanthate photofragmentation spectra which are assigned to S_2 (Figure 4C and top trace of Figure 6). A similar control study of OCS did not give S_2 emission. These results on Ni and Pd xanthate complexes are consistent with our recent gas-phase luminescence and mass spectroscopic studies on Zn xanthate compounds where S_2 and Zn metal are the major active species present during photodeposition.⁴

There are other possible routes for the formation of metal sulfide, one of which involves the loss of ROCS to produce LMS ($\text{M} = \text{Pd}, \text{Ni}$; $\text{L} = \text{S}_2\text{COCHMe}_2$), i.e., MS coordinated by one xanthate ligand as a first step. Loss of another xanthate ligand from this species would produce metal sulfides as final products. However, our detection of metal atoms and S_2 by emission spectroscopy supports the mechanistic pathway proposed in Figure 7.

Conclusions

We demonstrate that NiS and PdS films can be prepared photochemically under mild conditions from a single-source precursor with purity comparable to that of thermally grown films. The films grown by the thermal process have a relatively rough surface and are highly oriented polycrystalline, while those grown by the photolytic process are very smooth and either nonoriented polycrystalline (PdS) or nondiffracting (NiS) materials. Also, it is of interest that the deposits are obtained only on a selected area of the substrate irradiated by the laser beam.

Our *in situ* gas-phase luminescence measurements show the presence of atoms (Ni, Pd) and S_2 in the gas phase during photodeposition. The results indicate that the deposition process is initiated by the absorption of light by the gas-phase molecules and involves photochemical components. These are possibly followed by further thermal and photolytic processes on the surface and finally result in the formation of metal sulfide thin films.

Acknowledgment. This work was supported by the National Science Foundation (CHE-9509275). We thank James Ren (UCLA) for the XPS analyses and Dr. Kin-Man Yu (Lawrence Berkeley National Laboratory) for RBS measurements of the samples.

CM960589U

(26) Sapers, S. P.; Andraos, N.; Donaldson, D. J. *J. Chem. Phys.* **1991**, *95*, 1738.

(27) *JCPDS Powder Diffraction File*; McClune, W. F., Ed.; International Center for Diffraction Data: Swarthmore, PA, 1990.

(25) Jørgensen, C. K. *Inorganic Complexes*; Academic: New York, 1963; Chapter 7.